

Influence of Size and Orientation of 3D Printed Fiber on Mechanical Properties under Bending Stress

David Juracka^{1*}, Marek Kawulok¹, David Bujdos², Martin Krejsa¹

¹ Department of Structural Mechanics, Faculty of Civil Engineering, VSB-Technical University of Ostrava, Ludvika Podeste 1875/17, 708 00 Ostrava-Poruba, Czech Republic

² Department of Building Materials and Diagnostics of Structures, Faculty of Civil Engineering, VSB-Technical University of Ostrava, Ludvika Podeste 1875/17, 708 00 Ostrava-Poruba, Czech Republic

* Corresponding author, e-mail: david.juracka@vsb.cz

Received: 05 January 2022, Accepted: 13 June 2022, Published online: 08 July 2022

Abstract

The principle of FFF/FDM (Fused Filament Fabrication/Fused Deposition Modeling) 3D printing technology is the melting and application of a continuous fiber made of thermoplastic material, according to predefined routes on the substrate. A layer is created on which other layers are placed until the object is finished. It is the orientation of these fibers that greatly affects the resulting mechanical properties. Therefore, the printed object behaves orthotropic. The material does not blend perfectly or evenly between the individual fibers, which is why the resulting strength is limited by adhesion. Within the fibers themselves, it is also its dimension that affects the size of the contact surface and therefore the effect of adhesion. This contribution aims to compare the effect of fiber size in a given direction and its rotation in 3-point bending according to the standard ČSN EN ISO 178. The maximum bending load force was obtained and the bending stress and modulus of elasticity were determined. The influence of layer cohesion on the failure of the specimens is compared. One of the other important studied aspects for the effective production is the printing time of each specimen.

Keywords

3D printing, FFF, FDM, PETG, bending, nozzle

1 Introduction

3D printing technology is relatively new (1980 - the first patent attempt [1] by Hideo Kodama), yet widespread in many fields. Its capabilities apply mainly to the development of prototypes, such in engineering, medicine, the design industry, and even the fashion sector [2]. Nowadays, it also has a place in construction industry, where it can be used to print some kinds of structures, e.g., a smaller residential house from a special concrete mix [3]. Some research deals with the use of printed plastic structure, which is further used as reinforcement or lost formwork for concrete parts of structures [4, 5].

The resulting mechanical properties of the 3D printed objects depend on many aspects, e.g., direction and size of fibers, orientation of an object, printing temperature, material. These aspects affect its manufacturability, speed, material consumption, time, and especially its strength.

The author's whole research project intends to explore the possibilities of optimizing 3D printed elements produced by FFF (Fused Filament Fabrication) technology or otherwise

called FDM (Fused Deposition Modeling). The principle is the printing of a molten continuous fiber made of thermoplastic material, which is applied using a movable print head according to preset trajectories at one height level, which is called a layer. Then, another and another layers are applied to create the whole object. Article [6] describes the way in which the molten material of the individual fibers is interconnected and the size of their contact area. The cross-section of an element cannot be considered homogeneous because there are gaps between the individual fibers. For this reason, the elements have an orthotropic character, and therefore it is important to specify if the stress is conducted along the fibers, across, or at a certain angle [7–9]. The mechanical properties of these elements are further influenced by the used material, the temperature of the nozzle and the printing plate, the layer thickness, the fiber width and the adhesion of the fibers. It is also necessary to consider the internal filling of the object consisting of the geometric pattern and the percentage of filling in the defined space [10].

This paper aims to compare the effect of the fiber thickness, the effect of adhesion, and printing time on the mechanical properties determined by the three-point bending test according to the standard [11]. The maximum normal stress and the modulus of elasticity in tension and compression are calculated. The determined material characteristics will serve for further follow-up research on the optimization of elements cross-sections printed by a 3D printer and as input data for numerical modeling.

2 Specimen preparation

PETG, which is abbreviated as polyethylene terephthalate with modified glycol, was chosen for testing. Compared to other materials such as the often-used PLA (Polylactic acid) or ABS (Acrylonitrile butadiene styrene), it excels in higher adhesion between fibers and layers, toughness and higher melting point. It is generally used for mechanical components. The specimens were processed on the Prusa i3 MK3S+ 3D printer with PrusaSlicer preparation software [12].

When the fiber is applied to the substrate or layer, it acquires its characteristic cross-sectional shape (Fig. 1). Its width is largely determined by the diameter of the used nozzle; however, another influencing aspect is the amount of material flow. This continuously variable extrusion width can achieve gradient infill density, which can be used as one of the optimization factors [13].

Its height is generally around half of the width. On the contrary, the width can be changed during the preparation in the software. The detail and error-free printing depend on this value. To determine the effect and compare the behavior

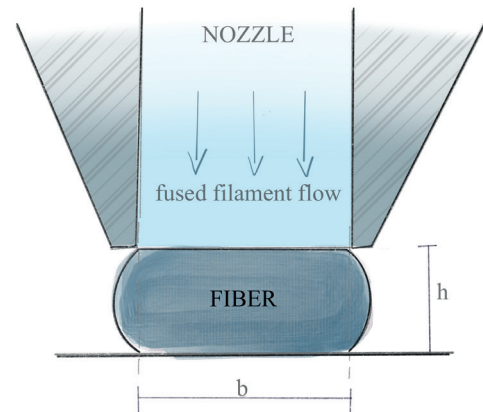


Fig. 1 Illustration of the cross-section of fiber printed by a nozzle

when using different fiber sizes, 2 categories were selected - a nozzle with a diameter of 0.4 mm (fiber height 0.2 mm) and 0.8 mm (height 0.4 mm). Therefore, the categories are marked as N 0.4 and N 0.8.

When testing the mechanical properties of orthotropic material, it is necessary to test the specimen for each direction of the fibers separately, and also to take into account the rotation of the fiber. Four sets of specimens (A, B, C, D) were created for each category. Fig. 2 illustrates the direction of the layers according to the orientation of the specimen. Fibers are placed along the longitudinal axis of the specimen in sets A and B, and perpendicularly to the axis in sets C and D. The dimensions of the specimen were selected and adjusted according to the standard CSN EN ISO 178 as 80 mm in length, 25 mm in width, and 15 mm in height. Five specimens with a given fiber direction were made for each set. Therefore, twenty samples were tested in total for each category (N 0.4 and N 0.8).

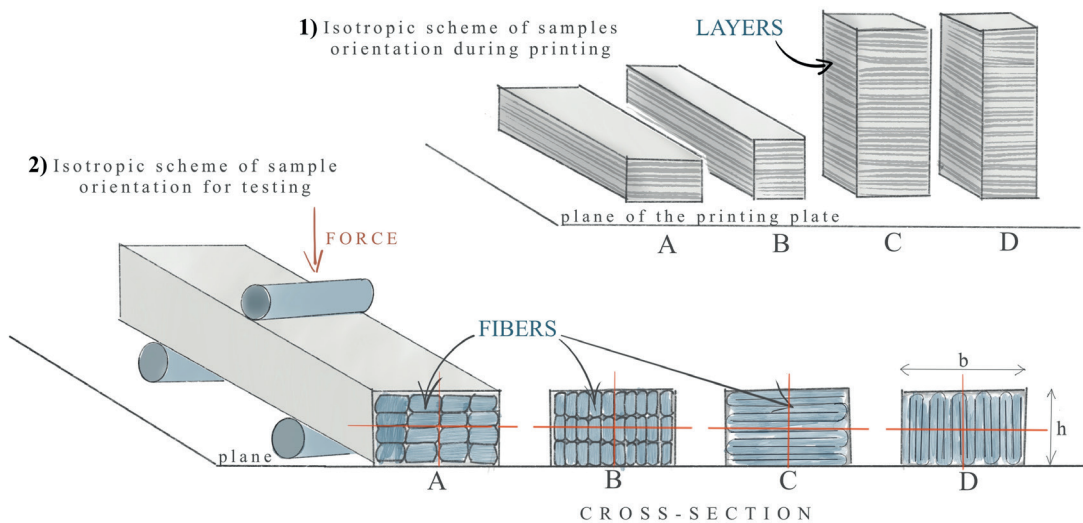


Fig. 2 Fiber and layer distribution test sets: 1) isotropic scheme - sample orientation when printing on a printing plate; 2) cross-section of the specimen - fiber orientation; A-Longitudinal orientation of fibers with a horizontal cross-section; B-Longitudinal orientation of the fiber with the cross-section standing upright; C- transverse orientation of fibers with a horizontal cross-section; D-transverse orientation of fibers with a cross-section upright

For each specimen, a full straight fill with a uniform fiber direction was chosen according to the set. A gcode file was generated from the preparatory software to instruct the 3D printer.

3 Methodology

Tests and calculations for three-point bending were performed according to the standard [11]. The diagram in Fig. 3 shows a schematic arrangement of the test body in the measuring system. Fig. 4 is a photograph showing the applied test according to the previous scheme in test device FP 10.

3.1 Maximum normal bending stress

The purpose of the test is to determine the maximum possible force $F(N)$ to bend the specimen, and then the value of the maximum normal bending stress σ_{fM} (MPa) can be calculated:

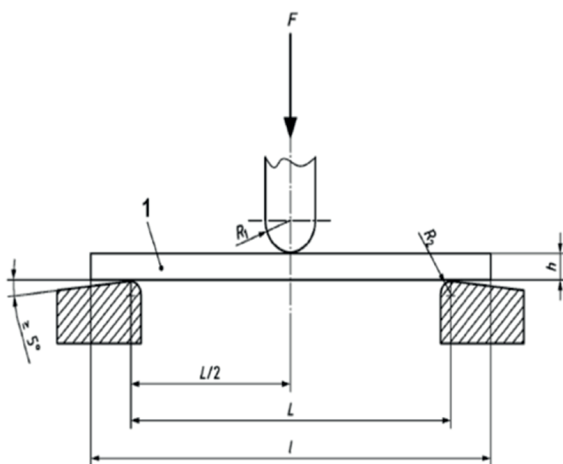


Fig. 3 Experimental setup of the three-point bending test [11]

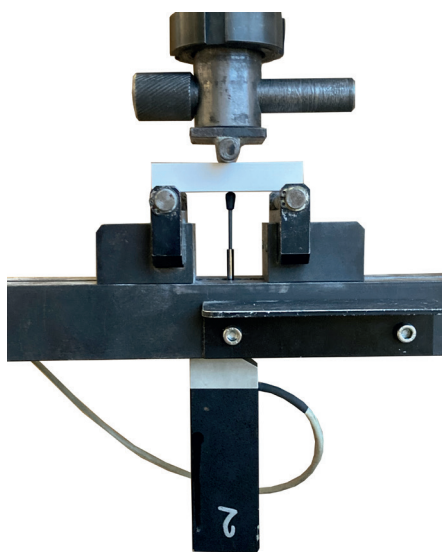


Fig. 4 Position of the specimen at the beginning of the test

$$\sigma_{fM} = (3FL) / (2bh^2), \quad (1)$$

where L is the seating of the abutment surfaces (mm), b is the width of the test piece (mm), and h is the thickness of the test specimen (mm).

3.2 Modulus of elasticity in flexure

In order to determine the linear approximated dependence between stress and strain, it is necessary to determine the flexural modulus. Therefore, the deflections s_1 and s_2 corresponding to the given bending deformation values are calculated according to the standard for the strains $\epsilon_{f1} = 0.0005$ and $\epsilon_{f2} = 0.0025$. When evaluating the results of the finished experiments, same misleading data were found at the beginning of the test for all specimens. The data relates to the values from the deformation sensor, which were caused by the abutment of the entire test device and the specimen. Hence, it was not possible to use the standard values of ϵ_{f1} and ϵ_{f2} , and the nearest usable strain values were found instead by using $\epsilon_{f1} = 0.005$ and $\epsilon_{f2} = 0.01$.

$$s_i = (\epsilon_{fi} L^2) / (6h), \quad (2)$$

where ϵ_{fi} is corresponding flexural strain (-), L is the seating of the abutment surfaces (mm), s is the corresponding deflection (mm), h is the thickness of the test specimen (mm).

For our individual specimen with its dimensions, described in paragraph 2, the resulting sought deflection values are:

- $s_1 = 0.228$ mm
- $s_2 = 0.445$ mm

Modulus of elasticity in flexure E_f (MPa):

$$E_f = (\sigma_{f2} - \sigma_{f1}) / (\epsilon_{f2} - \epsilon_{f1}). \quad (3)$$

4 Results

Four sets with five specimens each were tested in both categories (N 0.4 and N 0.8). Fig. 5 shows resulting load-displacement curves of representative specimens for each set and a comparison of using a 0.4 mm and 0.8 mm nozzle.

One should notice that category N 0.8 was able to transmit higher applied forces than category N 0.4 in each set. It turned out that the course of the test is very similar in each set between categories; the specimens was failing in the same way. For set A, after reaching the maximum force, the deformations increased with decreasing load (Fig. 5). Set B reached similar values as set A, but with a sharp drop of force with the same increase in deflection after reaching the maximum force. Sets C and D had a linear increase in

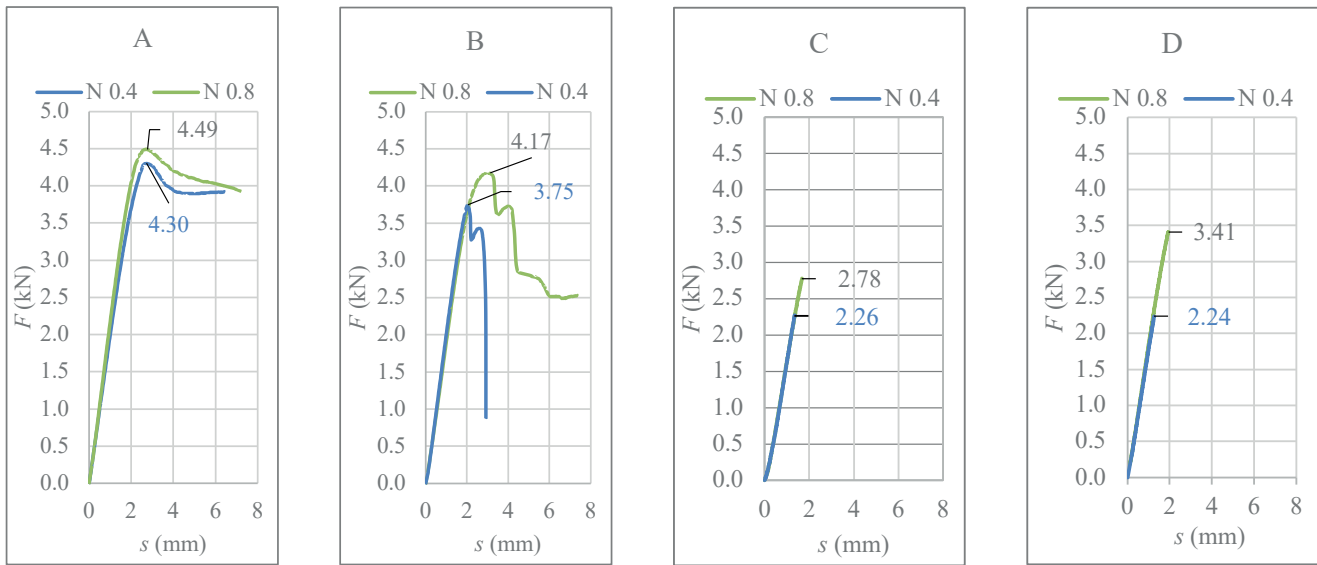


Fig. 5 Load-displacement diagrams - comparison of selected representative results between categories and sets of specimens

values and all specimens broke when a certain load value was reached. Both of these sets achieved higher values for category N 0.8 than category N 0.4.

Set A did not show any sample failures during the test, when there was only a gradual increase in deformation. For set B the layers were delaminated in all specimens of category N 0.4. Figs. 6 and 7 show photographs of representative specimens of the category after completion of the test. In category N 0.8 were two specimens also delaminated and the other two have quite similar progress as set A with increasing deformation without delamination.

The last test specimen of set B failed almost at the strength limit, which could be due to a manufacturing defect.

Delamination happened due to the insufficient adhesion between the fibers, which had the greatest effect during this rotation of the cross-section (Fig. 2) of the fiber and therefore can be considered as a limiting factor. The rotation of the fibers caused that the contact area in the direction of the load was smaller. In this case, the use of a larger nozzle, which doubles this size with a lower number of fibers, increases the chance to prevent delamination. Therefore, even larger nozzle sizes may be considered. In sets C and D, in all cases, the specimen completely broke before the possible strength limit was reached. Adhesion has become a limiting factor. However, this time the size of nozzle has a much greater effect.

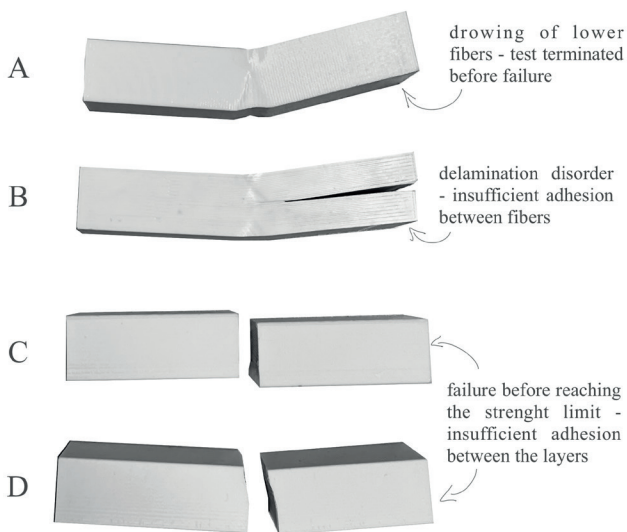


Fig. 6 Representative specimens of category N 0.4 after the 3-point bending test

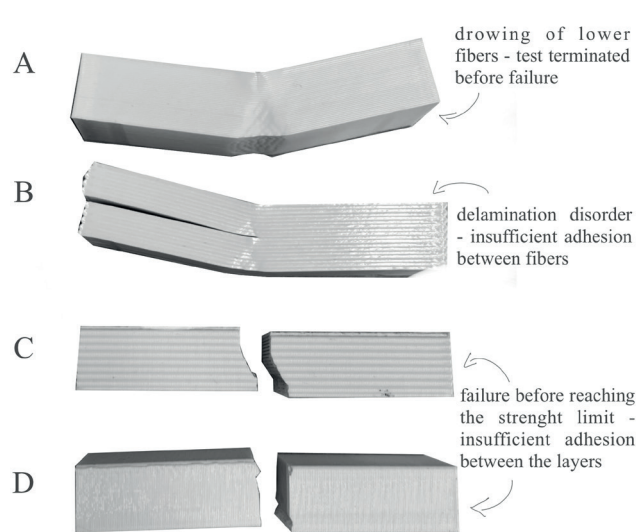


Fig. 7 Representative specimens of category N 0.8 after the 3-point bending test

The resulting maximum normal bending stress σ_{fM} (MPa) of the individual sets of specimens can be shown in Fig. 8.

As can be seen in the diagrams, the results show that sets A and B have reached the highest strength, and the effect of the fiber size was negligible. In the case of sets C and D, the size and direction of the fiber cross-section have a great influence. Although the specimen in set D reached the lowest value in the class N 0.4, with a twice as large nozzle the strength increased almost two times. The phenomena can be explained by larger contact area and better adhesion during manufacturing.

The modulus of elasticity in flexure is depicted in Fig. 9.

In the case of the modulus of elasticity in flexure, it seems there is no simple explanation of the results. In general, it can be seen that higher values can be achieved when longitudinal fibers are used (sets A and B). In the case of sets A, C and D, the values are higher for the class N 0.8. However, the results of set B show the opposite trend.

The comparison of the printing time of one specimen from a given set is also quite interesting (see Fig. 10). Category N 0.8 always achieves a much shorter time to produce the specimen. It may be an important aspect of production because with twice the nozzle size, up to three times shorter production times can also be achieved with higher strength values. One should notice, that with a longitudinally oriented fiber, it is possible to accomplish higher efficiencies than with a transverse orientation.

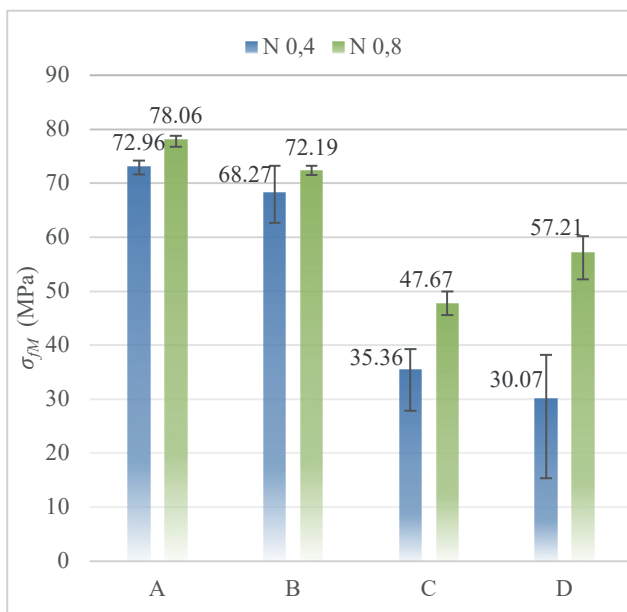


Fig. 8 Comparison of the maximum normal bending stress between categories and sets of specimens with error bars

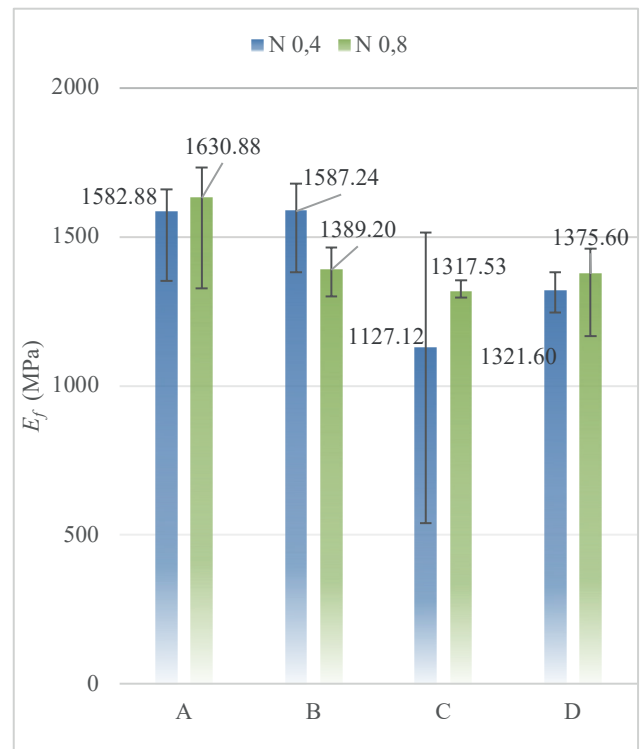


Fig. 9 Comparison of the modulus of elasticity in flexure between categories and sets of specimens

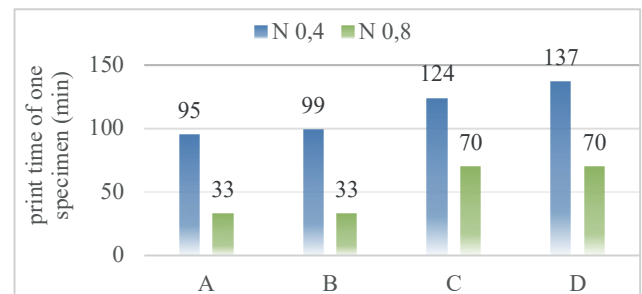


Fig. 10 Comparison of the printing time between categories and sets of specimens

5 Conclusions

The purpose of the research was to investigate the effect of the fiber size, the size of the nozzle used and orientation of the layer on the mechanical properties of the specimens and their behavior in three-point bending. These properties were determined for two sizes of fiber and nozzle, and four different fiber orientations and rotations.

It has been shown that the greatest efficiency can be achieved in the longitudinal direction with horizontal cross-section rotation. In terms of the type of nozzle used, it was found out that there is no significant difference in the achieved strength in the case of set A and B, but the production time for a larger diameter of fiber was three times

quicker. All specimens showed stable behavior during the test, except set B in the category N 0.8, where differences in the type of specimen failure were observed.

The effect of adhesion has become a major limiting factor. The mere rotation of the fiber cross-section, although still a longitudinal orientation of the layers, causes delamination. Therefore, this aspect must be considered for further research. Despite the low adhesion, the specimens of set B achieved similar results in both categories.

Similar results were obtained using the perpendicular direction of the fibers. The limiting factor was adhesion as well, which in this case caused the specimens to fail before the strength limit was reached. However, in this case, the size of the fiber already had a major impact on the results. As the diameter of the nozzle increased twice, the contact area of the fibers also increased, which made it possible to achieve almost double strength by this printing method. However, it is still the least load-bearing and most time-consuming configuration for printing.

References

- [1] Kodama, H. "Stereoscopic figure drawing device Japan", Japan, JPS56144478A, 1980.
- [2] Končič, J., Ščapec, J. "3D print additive technology as a form of textile material substitute in clothing design – interdisciplinary approach in designing corsets and fashion accessories", *Industria Textila*, 69(3), pp. 190–196, 2018.
<https://doi.org/10.35530/IT.069.03.1430>
- [3] Ji, G., Ding, T., Xiao, J., Du, S., Li, J., Duan, Z. "A 3D Printed Ready-Mixed Concrete Power Distribution Substation: Materials and Construction Technology", *Materials*, 12(9), 1540, 2019.
<https://doi.org/10.3390/ma12091540>
- [4] Katzer, J., Sztatkiwicz, T. "Effect of 3D Printed Spatial Reinforcement on Flexural Characteristics of Conventional Mortar", *Materials*, 13(14), 3133, 2020.
<https://doi.org/10.3390/ma13143133>
- [5] Katzer, J., Skoratko, A. "Concept of Using 3D Printing for Production of Concrete–Plastic Columns with Unconventional Cross-Sections", *Materials*, 14(6), 1565, 2021.
<https://doi.org/10.3390/ma14061565>
- [6] Garzon-Hernandez, S., Garcia-Gonzalez, D., Jérusalem, A., Arias, A. "Design of FDM 3D printed polymers: An experimental-modelling methodology for the prediction of mechanical properties", *Materials & Design*, 188, 108414, 2020.
<https://doi.org/10.1016/j.matdes.2019.108414>
- [7] Ravindrababu, S., Govdeli, Y., Wong, Z. W., Kayacan, E. "Evaluation of the influence of build and print orientations of unmanned aerial vehicle parts fabricated using fused deposition modeling process", *Journal of Manufacturing Processes*, 34, pp. 659–666, 2018.
<https://doi.org/10.1016/j.jmapro.2018.07.007>
- [8] Wu, W., Geng, P., Li, G., Zhao, D., Zhang H., Zhao., J. "Influence of Layer Thickness and Raster Angle on the Mechanical Properties of 3D-Printed PEEK and a Comparative Mechanical Study between PEEK and ABS", *Materials*, 8(9), pp. 5834–5846, 2015.
<https://doi.org/10.3390/ma8095271>
- [9] Dizon, J. R. C., Espera Jr, A. H., Chen, Q., Advincola, R. C. "Mechanical characterization of 3D-printed polymers", *Additive Manufacturing*, 20, pp. 44–67, 2018.
<https://doi.org/10.1016/j.addma.2017.12.002>
- [10] Dudescu, C., Racz, L. "Effects of Raster Orientation, Infill Rate and Infill Pattern on the Mechanical Properties of 3D Printed Materials", *ACTA Universitatis Cibiniensis*, 69(1), pp. 23–30, 2017.
<https://doi.org/10.1515/aucts-2017-0004>
- [11] ISO "ISO 178:2019 Plastics - Determination of flexural properties", International Organization for Standardization, Geneva, Switzerland, 2019.
- [12] Prusa Research "Prusa Slicer 2.4.2" [software] Available at: https://www.prusa3d.com/page/prusaslicer_424/
- [13] Hermann, S. "Gradient Infill for 3D Prints", CNC Kitchen [online] Available at: www.cnckitchen.com/blog/gradient-infill-for-3d-prints